# Precision Sensorimotor Control in Aging Fragile X Mental Retardation 1 Gene Premutation Carriers

By



Walker S. McKinney
B.S, Northwestern University, 2017

Submitted to the graduate degree program in Clinical Child Psychology and the Graduate Faculty of the University of Kansas in partial fulfillment of the requirements for the degree of Master of Arts.

---

Chair: Matthew W. Mosconi, Ph.D.

---

Steven F. Warren, Ph.D.

---

Eric M. Vernberg, Ph.D., ABPP

Date Defended: 1 July 2019

The thesis committee for Walker S. McKinney certifies that this is
the approved version of the following thesis:

# Precision Sensorimotor Control in Aging Fragile X Mental Retardation 1 Gene Premutation Carriers

Chair: Matthew W. Mosconi, Ph.D.

Date Approved: 1 July 2019

## Abstract

Individuals with premutation alleles of the FMR1 gene are at risk of developing Fragile X-associated Tremor/Ataxia Syndrome (FXTAS), a neurodegenerative condition affecting sensorimotor, cognitive and psychological function. There is limited information on quantitative symptom traits in aging premutation carriers to assist in identifying neurodegenerative processes and understanding neurodegenerative mechanisms. 26 FMR1 premutation carriers ages 44-77 years and 31 age-matched healthy controls completed a visually guided precision gripping task in which they pressed with their thumb and forefinger against load cells while receiving visual feedback. Individuals maintained a constant force for 2- or 8- seconds. During initial pressing, reaction time, the rate at which individuals increased their force, and force accuracy were measured. During sustained gripping, the complexity of the force time series, force variability, and mean force were examined. At the end of each trial, the rate at which individuals decreased their force was measured. During initial pressing, premutation carriers, relative to controls, showed longer reaction times, particularly at younger ages. They also showed reduced rates of force generation and reduced accuracy relative to controls. During sustained force, premutation carriers demonstrated reduced force complexity, though this effect varied as a function of age and hand; it was reduced across ages for the non-dominant hand but was more severely reduced at younger ages for the dominant hand. Lower sustained force complexity was associated with greater cytosine-guanine-guanine (CGG) repeat length. Increased reaction time, increased sustained force variability, and increased rates of force relaxation each were associated with more severe clinically rated FXTAS symptoms. Findings of increased reaction time in premutation carriers implicate neurodegenerative processes affecting the ability to rapidly prepare the motor system for action. Premutation carriers also showed reduced accuracy of their

initial force output indicating impairments precisely planning rapid motor behavior. Reduced complexity of sustained motor output suggests deficits in reactively adjusting motor behavior in response to sensory feedback. Overall, these results indicate that sensorimotor issues in aging premutation carriers affect multiple motor systems, and quantitative tests of precision visuomotor ability may serve as key targets for monitoring FXTAS risk and progression.

*Keywords***:** Fragile X-associated tremor/ataxia syndrome, FMR1 premutation, sensorimotor, precision grip, neurodegeneration, bradykinesia, dysmetria

Table of Contents

# List of Figures

# List of Tables

# Precision Sensorimotor Control in Aging Fragile X Mental Retardation 1 Gene Premutation Carriers

Fragile X is the most common heritable form of intellectual disability, and it is caused by "full" mutations of the *FMR1* gene consisting of >200 cytosine-guanine-guanine (CGG) repeats (Kremer et al., 1991; Verkerk et al., 1991; Yu et al., 1991). Premutations of the *FMR1* gene involving 55-200 CGG repeats also confer risk for multiple subclinical issues as well as medical, psychiatric, and neurodegenerative conditions (Lozano, Rosero, & Hagerman, 2014) including fragile-X associated tremor/ataxia syndrome (FXTAS). FXTAS is a neurodegenerative disease in which patients present with a variety of motor, cognitive, psychiatric and medical issues, as well as cerebellar and cortical degeneration typically beginning at ages 50-70 years (Brunberg et al., 2002; Jacquemont et al., 2003). The defining clinical symptoms of FXTAS include intention tremor, gait ataxia, and Parkinsonism (Hagerman et al., 2001; Jacquemont et al., 2003; Juncos et al., 2011; Leehey et al., 2007), though some patients demonstrate severe decline in cognitive processes or the development of psychiatric issues (Grigsby et al., 2008). Pathology of the middle cerebellar peduncle (MCP sign), cerebral atrophy, and intranuclear inclusions also are associated with FXTAS (Brunberg et al., 2002; Greco et al., 2006). Still, symptom presentation is highly variable across patients, and objective, quantitative tools are needed to identify aging premutation carriers most at risk of developing FXTAS, track disease progression, and determine central mechanisms (Jacquemont et al., 2004; Leehey et al., 2007).

Prior quantitative studies have indicated that premutation carriers with FXTAS and elderly, asymptomatic premutation carriers each show sensorimotor issues. For example, FXTAS patients show increased postural sway relative to healthy aging individuals (Aguilar et al., 2008), while aging premutation carriers with and without FXTAS each have shown greater postural

sway during standing associated with greater CGG repeat length (Kraan et al., 2013; O'Keefe et al., 2015; Wang, Khemani, Schmitt, Lui, & Mosconi, 2019). Studies of fine motor abilities critical to everyday activities have indicated that asymptomatic *FMR1* premutation carriers (Shickman et al., 2018) and FXTAS patients (Schneider et al., 2012) show reduced motor planning speed. Park and colleagues also reported increased force variability during sustained finger abductions suggesting alterations in the ability to reactively adjust precision motor behavior in response to sensory feedback (Park et al., 2019). Importantly, Shickman and colleagues documented that more severe fine motor issues were associated with greater CGG repeat length in asymptomatic aging premutation carries, suggesting fine motor deficits may covary with FXTAS risk (Shickman et al., 2018). While these studies indicate tests of fine motor control may be useful for quantifying clinical and subclinical issues in aging premutation carriers, precise and translational measurements of multiple fine motor processes, including the initiation, maintenance, and termination of behavior, are needed to define affected systems, clarify neurobiological mechanisms of FXTAS, and monitor both disease risk and progression.

One candidate approach for characterizing the multiple fine motor processes associated with FXTAS is studying visually guided precision gripping. Precision gripping is important for many daily living activities (e.g., writing, grasping objects), and multiple studies have documented atypical precision gripping behavior in neurodevelopmental (Mosconi et al., 2015; Wang et al., 2015) and neurodegenerative conditions that affects patients' quality of life (Vaillancourt, Slifkin, & Newell, 2001a). Further, the neural bases of visually guided precision gripping have been studied extensively suggesting that clarifying spared and affected processes may help identify brain mechanisms in patient populations (Ehrsson et al., 2000; Kuhtz-Buschbeck et al., 2008; Neely, Coombes, Planetta, & Vaillancourt, 2013; Prodoehl, Corcos, &

Vaillancourt, 2009). During precision gripping, individuals initiate a "rise phase" in which they rapidly increase their force output to reach a target level. Initial pressing is characterized by a transient force overshoot reflecting afferent delay of sensory feedback information (Desmurget et al., 1999; Potter, Kent, Lindstrom, & Lazarus, 2006). During a subsequent "sustained phase", individuals aim to maintain a relatively constant level of force integrating feedforward and sensory feedback processes. Greater variability in force and reduced complexity of the force time series are seen in multiple patient populations and implicate failures in the ability to dynamically and reactively adjust precision motor output in response to sensory feedback (Chu & Sanger, 2009; Vaillancourt, Slifkin, & Newell, 2001b). At the end of precision gripping actions, participants engage in a "relaxation phase" in which they rapidly release their grip force.

In the present study, we characterized visually guided precision gripping behavior across rise, sustained and relaxation phases in *FMR1* premutation carriers ages 44-77 years. Our primary goal was to characterize precision visuomotor behaviors in aging *FMR1* premutation carriers. By examining a large age range, we were able to determine whether visually guided precision gripping issues were more prominent at relatively earlier stages of aging suggesting that they may be prodromal markers of degeneration, or whether they may become more prominent later suggesting decline at advanced ages. Gripping was tested across both hands to determine if neurodegenerative processes associated with aging in premutation carriers may be lateralized as previously suggested (Przybyla, Haaland, Bagesteiro, & Sainburg, 2011; Raw, Wilkie, Culmer, & Mon-Williams, 2012). We also examined the relationship between visuomotor outcomes, FXTAS clinical symptoms, and CGG repeat length to determine the utility of our measures for objectively characterizing neuromotor degeneration associated with the severity of and risk for FXTAS.

# Methods

## Participants

Twenty-six premutation carriers and 31 controls completed visuomotor testing (Table 1). No premutation carriers had an existing diagnosis of any neurological disorder, nor did they self-report any motor (e.g., gait ataxia, intention tremor) or memory issues. Controls were excluded for current or past neurodegenerative, neurological, or major psychiatric disorders (e.g., schizophrenia, bipolar disorder). Controls also were excluded for a family history of fragile X syndrome or intellectual/developmental disabilities in first- or second-degree relatives. Participants were excluded if they reported any neurological or musculoskeletal disorder that could potentially cause atypical motor functioning or a history of medications known to affect motor functioning, including antipsychotics, stimulants, or benzodiazepines (Reilly, Lencer, Bishop, Keedy, & Sweeney, 2008).

*FMR1* premutation carriers were identified through local fragile X clinics and postings on local and national fragile X association listservs. Control participants were recruited through community advertisements. This study was carried out in accordance with the recommendations of and was approved by the University of Texas, Southwestern Institutional Review Board. All subjects provided written informed consent after a complete description of the study in accordance with the Declaration of Helsinki.

## Neurological and Radiological Evaluations

*FMR1* premutation carriers completed a clinical exam by a neurologist with expertise in movement control in aging (Pravin Khemani). The clinical exam included administration of the International Cooperative Ataxia Rating Scale (Trouillas et al., 1997). The ICARS is comprised of 19 sections examining postural and gait disturbances, ataxia, dysarthria and oculomotor

behavior. Higher scores indicate more severe neuromotor issues. The ICARS has been validated previously for diagnosis of ataxia in patients with focal cerebellar lesions (Schoch et al., 2007), hereditary spinocerebellar and Friedrich's ataxia (Schmitz-Hubsch et al., 2006).

Sixteen *FMR1* premutation carriers also underwent a T2-weighted MRI scan (repetition time = 6350 msec; echo time = 100 msec; flip angle = 120º; field of view = 256 × 156 × 256mm$^3$; 78 axial slices; 1 × 1 × 2mm$^3$ voxels; no gap) to test for presence of the MCP sign, cerebral atrophy or hyperintensities, or other cerebral, brainstem, or cerebellar alterations consistent with a diagnosis of FXTAS (Jacquemont et al., 2003).

**Visuomotor Testing**

Participants completed two tests of visuomotor behavior differentiated by the trial duration ("pulse" trials were 2-sec and "sustained" trials were 8-sec). For both tests, stimuli were presented on a 102 cm (40 inches) Samsung LCD monitor with a resolution of 1366 ×768 and a 120 Hz refresh rate. Participants were tested in a darkened room while seated 52 cm from the display monitor with their elbow at 90° and their forearm resting in a relaxed position on a custom-made arm brace. The arm brace was clamped to a table to keep the participant's arm position stable throughout testing (Figure 1). The participant's hand was pronated and lay flat with digits comfortably extended. Participants used their thumb and index finger to press against two opposing precision load cells (ELFF-B4-100N; Entran) 1.27 cm in diameter secured to a custom grip device attached to the arm brace. A Coulbourn (V72-25) resistive bridge strain amplifier received analog signal from the load cells. Data were sampled at 200 Hz with a 16-bit analog-to-digital converter (DI-720; Dataq Instruments). Data were converted to Newtons of force using a calibration factor derived from known weights before the study (Mosconi et al., 2015).

**Procedures**

Before testing, each participant's maximum voluntary contraction (MVC) was calculated separately for each hand using the average of the maximum force output during three trials in which participants pressed as hard as they could for three seconds.

During visuomotor testing, participants viewed a horizontal white force bar that moved upward with increased force and downward with decreased force and a static target bar that was red during rest and turned green to cue the participant to begin pressing at the beginning of each trial (Figure 2). Participants received two instructions: (1) press the load cells as quickly as possible when the red target bar turns green, and (2) keep pressing so that the force bar stays as steady as possible at the level of the green target bar. These instructions were identical for the two versions of the task described below.

"Pulse" (2-second) and "sustained" (8-second) trials were administered at 15%, 45%, and 85% of each individual's MVC. During the pulse test, two blocks of five trials were presented for each hand at each force level (2 hands x 3 force levels x 2 blocks x 5 trials = 60 pulse trials). Each 2-s pulse trial alternated with 2-s rest periods. A 15-s rest block was provided after each block of trials. During the sustained test, participants completed two blocks of three trials for each hand at each force level (2 hands x 3 force levels x 2 blocks x 3 trials = 36 sustained trials). Eight-second trials were followed by 8-s rest periods, and each block was separated by 15-s of rest. For both tests, the same hand was never tested on consecutive blocks. The order of force levels was randomized across blocks. The order of the two experiments was randomly assigned to each participant. Participants self-reported their handedness.

**Visuomotor Data Processing**

Force traces for each trial were low-pass filtered via a double-pass 4th-order Butterworth filter at a cutoff of 15 Hz in MATLAB. Data were analyzed using custom MATLAB scripts previously developed by our lab (Wang et al., 2015).

Data from three distinct phases were analyzed. During the initial *rise* phase in which individuals pressed on the load cells to reach the target level, force level is guided primarily by feedforward processes completed prior to the availability of visual and other sensory feedback processes to guide force output (Ghez, Hening, & Gordon, 1991; Prablanc & Martin, 1992). We examined the latency to rise onset, peak rate of force increase (i.e., the maximum value of the first derivative of the force trace), duration of the rise phase, and accuracy of the rise phase. The onset of the rise phase was calculated as the time at which the rate of force increase first exceeded 5% of the peak rate of force increase and remained above this level for at least 100ms (Grafton & Tunik, 2011; Wang et al., 2015). Reaction time was calculated as the difference between rise phase onset and the appearance of the start cue. The rise phase offset was calculated as the time-point when the rate of force increase fell below 5% of the peak rate of force increase, and the force level was within 90% to 110% of the mean force of the sustained phase (Wang et al., 2015). The peak rate of force increase was defined as the maximum value of the first derivative of the force trace. Rise phase duration was then calculated as the difference between the rise phase offset and rise phase onset. Due to the known effect of participant MVC on peak rate of force increase and rise phase duration (i.e., rate of force generation and duration both increase asymptotically with increases in force output), rate of force increase and duration of initial force output were analyzed relative to MVC (i.e., rate of force increase/MVC; rise phase duration/MVC). Finally, force accuracy for the rise phase was calculated as the force at rise offset divided by the target force (i.e., $Rise\ Accuracy = \frac{(F_{rise})}{(F_{target})}$). Values below 1 represent an

undershooting of the target force and values above 1 reflect overshooting of the target force. An accuracy score of 1 would indicate perfect accuracy. The entire rise phase was excluded if participants began gripping before the start cue, or if they returned to baseline prior to reaching 90% of the target force. Rise phase data for both the pulse and sustained tasks were analyzed within the same model to allow for the analysis of a task effect (i.e., pulse vs. sustained).

To determine the extent to which participants could maintain a constant level of force, the *sustained* phase was examined and defined as the period following rise phase offset and prior to the appearance of the stop cue. Due to the brief duration of pulse trials in which force levels are highly variable, only 8-s trials were used to examine the sustained phase. The mean force of the time series was calculated to determine individuals' ability to complete the task. The variability of the force time series was calculated using the following procedures: first, force data were linearly detrended to account for systematic changes in mean force over the course of the trial (e.g., data drift). Second, the within-trial standard deviation (SD) of the force time series was calculated. To examine the time-dependent structure of the time series, the approximate entropy (ApEn) was calculated for each trial (Mosconi et al., 2015; Pincus & Goldberger, 1994; Slifkin & Newell, 1999; Vaillancourt et al., 2001b). ApEn returns a value between 0 and 2, reflecting the predictability of future values in a time series based on previous values. For example, a sine wave has accurate short- and long-term predictability, corresponding to an ApEn value near 0. High irregularity of the data, reflective of the independence of each force value, returns an ApEn near 2. The algorithm and parameter settings for these calculations ($m = 2$; $r = 0.2 \times$ standard deviation of the signal) were identical to previous work (Vaillancourt & Newell, 2000). Sustained phase variables were excluded if fewer than 4 seconds of data were available or if participants returned to baseline for more than 1 second (e.g., a > 1 sec dip of the force signal).

In order to determine the rate at which individuals released force at the end of trials, the *relaxation* phase also was examined. The onset of the relaxation phase was defined as the first point following the stop cue (target bar turned red) at which velocity (i.e., rate of change of force) went below 5% of the peak velocity and remained at that level or below for at least 100ms. The offset of the relaxation phase was defined as the first point at which velocity rose back above 5% of the peak relaxation velocity. We examined the rate of force decrease during the relaxation phase. The peak rate of force decrease was identified as the minimum value of the first derivative of the force trace following the stop cue. Again, due to the potential impact of participant MVC on peak rate of force decrease, this measurement was then divided by MVC. Thus, relaxation data is relative to each participant's individual strength. Relaxation phases were not included if the participant released force prior to the stop cue. Relaxation phase data for both the pulse and sustained tasks were analyzed within the same model to allow for the analysis of a task effect (i.e., pulse vs. sustained).

**CGG Repeat Count**

All premutation carriers provided blood samples to confirm premutation status. *FMR1* CGG repeat count was quantified using molecular testing conducted at Dr. Elizabeth Berry-Kravis' Molecular Diagnostic Laboratory at Rush University. Genomic DNA was isolated from peripheral blood leukocytes samples. The *FMR1* polymerase chain reaction (PCR) test with quantification of allele-specific CGG repeat count was performed using commercially available kits (Asuragen, Inc., Austin, TX). For women, CGG repeat analyses reflect the longest CGG repeat of the two alleles.

**Cognitive Measures**

Cognitive functioning was assessed using the abbreviated battery of the Stanford-Binet Intelligence Scales, Fifth Edition (SB-5) including nonverbal fluid reasoning and verbal knowledge sub-sections (Roid, 2003). One participant did not complete the SB-5 due to not being fluent in English.

**Statistical Analyses**

To determine whether visuomotor ability differed according to premutation carrier status and to determine if the relationship between age and visuomotor outcomes varied as a function of group, general linear multilevel mixed effect (MLM) analyses were conducted. This approach allows for the simultaneous examination of within- and between-subject fixed effects while allowing within-subject factors to differ for each participant as random effects. Additionally, these analyses allowed for the analysis of interactions within the repeated measures design without listwise deletion of participant data (e.g., if a participant had a shortened testing session and only completed the task with one hand). Task/condition effects (percent MVC, hand, task) were identified as level 1 predictors and subject effects (group, age) were identified as level 2 predictors. Random variance components for the intercept (subject) and the slope of target force level (percent MVC) also were analyzed. To maintain relatively parsimonious models, the four- and five-way interaction between factors were not analyzed. Initial models included all two- and three-way interactions, after which variables and interactions were removed and model fit was compared between the previous and current models using a likelihood ratio test. Only variables which significantly ($p < .05$) improved model fit were incorporated into the final models. All model predictors were centered. Mixed effect modeling was conducted using the *lmer* package within R version 3.4.4.

Due to the non-normal distribution of CGG repeat length and ICARS scores, the relationships between visuomotor outcomes, ICARS scores, and CGG repeat length were examined using Spearman's rank-order correlations. Linear regression was used to determine if total ICARS scores were related to age, CGG repeat length, or the interaction of age and CGG repeat length. Due to the large number of correlations that were performed, only results with $p < .01$ were interpreted as significant. Correlational and regression analyses were conducted using IBM SPSS Statistics 25.

## Results

### Demographics

Healthy controls had significantly higher full-scale IQs ($M$ = 109.3, $SD$ = 12.8) than premutation carriers ($M$ = 99.5, $SD$ = 12.1), $t(54) = 2.93$, $p < .01$, though IQ was in the average range for both groups (Table 1). Controls and carriers did not differ on age, sex ratio, or handedness. Nine premutation carriers did not complete the clinical evaluation due to scheduling difficulties. For the 17 premutation carriers who completed the clinical visit, ICARS scores are presented in Table 1. Increased age was significantly associated with increased ICARS scores ($F(1,15) = 9.858$, $p = .007$, $R^2 = .397$). The addition of CGG repeat length to this model did not significantly improve fit ($F\Delta(1,14) = 1.891$, $p = .191$, $R^2\Delta = .072$), nor did the interaction between age and CGG repeat length ($F\Delta(1,13) = .515$, $p = .486$, $R^2\Delta = .020$).

### MVC

Premutation carriers and controls did not differ on MVC ($\beta$ = -6.222, $SE$ = 7.368, $p$ = .402). No lateralized differences in MVC between groups were seen (group x hand: $\beta$ = 7.303, $SE$ = 3.971, $p$ = .072).

### Rise Phase

Fixed effect estimates and random effect variances as well as their associated standard error values for rise phase models are presented in Tables 2 (reaction time and initial rate of force increase) and 3 (duration and accuracy).

Participants showed shorter reaction times during the pulse task relative to the sustained task ($\beta$ = 0.086, *SE* = 0.012, $p < .001$). Additionally, reaction time increased with increases in target MVC percent ($\beta$ = 0.072, *SE* = 0.014, $p < .001$) and age ($\beta$ = 0.049, *SE* = .023, $p = .034$). *FMR1* premutation carriers demonstrated longer reaction times than controls, especially at younger ages and during the pulse compared to the sustained task (Figure 3; group x task x age: $\beta$ = -0.099, *SE* = 0.028, $p < .001$).

Participants demonstrated a higher rate of force increase during the pulse compared to the sustained task ($\beta$ = -0.386, *SE* = 0.046, $p < .001$). Rate of force increase was greater at higher compared to lower MVC target levels ($\beta$ = 1.987, *SE* = 0.082, $p < .001$). Multiple three-way interactions were significant. For each of these interactions, premutation carriers showed a reduced rate of force increase relative to controls, but this was most severe at higher force levels of the pulse compared to the sustained task (Figure 4; group x task x percent MVC: $\beta$ = 0.625, *SE* = 0.217, $p = .004$), at younger ages and during the pulse compared to the sustained task (group x task x age: $\beta$ = -0.316, *SE* = 0.104, $p = .002$), and at younger ages and at higher percent MVC levels (group x percent MVC x age: $\beta$ = 0.339, *SE* = 0.169, $p = .049$).

For all participants, rise phase duration was greater during the pulse task compared to the sustained task ($\beta$ = -0.004, *SE* = 0.0003, $p < .001$) and scaled with target MVC level ($\beta$ = 0.001, *SE* = 0.0004, $p = .003$). Relative to controls, premutation carriers showed longer rise phase duration than controls, but only for their dominant hand (group x hand: $\beta$ = -0.002, *SE* = 0.0006, $p = .002$).

Participants overshot target force levels more during the rise phase of the pulse compared to the sustained task ($\beta$ = -0.015, *SE* = 0.004, $p < .001$). Specifically, participants initially overshot target force levels during the 15% MVC condition but not the 45% or 85% MVC conditions ($\beta$ = -0.075, *SE* = 0.008, $p < .001$). Premutation carriers showed increased target overshoot relative to controls that was more severe when they used their non-dominant hand during the pulse task (group x hand x task: $\beta$ = -0.033, *SE* = 0.016, $p = .044$) and when using the non-dominant hand at lower force levels (Figure 5; group x hand x percent MVC: $\beta$ = -0.047, *SE* = 0.020, $p = .017$).

**Sustained Phase**

The fixed effect estimates and random effect variances as well as their associated standard errors for all sustained phase models are presented in Table 4.

Participants demonstrated reduced ApEn at higher compared to lower target force levels ($\beta$ = -0.124, *SE* = 0.014, $p < .001$). Premutation carriers showed reduced ApEn relative to controls, but this group difference varied as a function of age and hand tested (Figure 6; group x hand x age: $\beta$ = -0.041, *SE* = 0.017, $p = .014$). Specifically, premutation carriers showed reduced ApEn across age for the non-dominant hand, but this effect was more severe at younger ages relative to older ages for the dominant hand.

Force SD scaled with target MVC level ($\beta$ = 3.348, *SE* = 0.477, $p < .001$), and force SD was greater for the non-dominant relative to dominant hand for participants ($\beta$ = 0.470, *SE* = 0.180, $p = .010$). There were no group differences or group interactions for force SD.

Mean sustained force scaled with target MVC level ($\beta$ = 54.478, *SE* = 2.371, $p < .001$). Compared to controls, premutation carriers demonstrated lower mean force with their dominant hand only (group x hand: $\beta$ = 3.480, *SE* = 0.988, $p < .001$).

### Relaxation Phase

At the end of trials, participants decreased their force level more rapidly during higher relative to lower target force levels ($\beta$ = 4.188, $SE$ = 0.098, $p < .001$) and during the pulse compared to the sustained force trials ($\beta$ = -0.203, $SE$ = 0.033, $p < .001$). There were no significant group differences or group interactions for rate of force decrease.

### Visuomotor Behavior and Clinical/Demographic Outcomes

**CGG repeat length.** The relationships between CGG repeat length and visuomotor behavior are presented in Table 5. Greater CGG repeat length was associated with reduced non-dominant hand ApEn in the 45% MVC condition (Figure 7A; $\rho$ = -.529, $p$ = .009). No other visuomotor variables were associated with CGG repeat length.

**Clinical symptoms.** The relationships between total ICARS scores and visuomotor behavior are presented in Table 6. More severe total ICARS scores were associated with greater reaction times during the pulse task in the dominant hand 15% MVC condition ($\rho$ = .774, $p$ = .003), dominant hand 85% MVC condition ($\rho$ = .724, $p$ = .008), and non-dominant hand 85% MVC condition (Figure 7B; $\rho$ = .795, $p$ = .002). More severe total ICARS scores also were associated with greater reaction times during the dominant hand 15% MVC condition of the sustained task ($\rho$ = .612, $p$ = .009). More severe ICARS scores were associated with higher force SD during the non-dominant hand 45% MVC condition (Figure 7C; $\rho$ = .663, $p$ = .004). Additionally, more severe total ICARS scores were associated with more negative (i.e., quicker) rates of force decrease during the relaxation phase of the pulse task dominant hand 15% MVC (Figure 7D; $\rho$ = -.827, $p < .001$) and 45% MVC conditions ($\rho$ = -.841, $p < .001$).

## Discussion

Despite sensorimotor impairments being central to the diagnosis of FXTAS, few studies have quantified precision sensorimotor behaviors in aging *FMR1* premutation carriers. Here, we examined multiple components of precision visuomotor behavior in aging premutation carriers, including initial force output, sustained precision motor behavior, and the rate of force termination. Five key findings are documented. First, younger premutation carriers demonstrated longer reaction times than controls indicating delays in generating visually cued motor behavior may be present during early stages of aging. Second, aging premutation carriers demonstrated a reduced ability to rapidly increase force during precision gripping, suggesting that initial motor output is slowed. Third, premutation carriers showed a larger overshoot of target force levels during initial force generation implicating reduced accuracy of internal action plans. Fourth, younger premutation carriers demonstrated reduced complexity of their sustained force output (i.e., ApEn), suggesting the ability to dynamically adjust motor output in response to sensory feedback may be impacted, especially during initial stages of aging during which premutation carriers first become vulnerable to FXTAS-associated deterioration. Last, multiple impairments of rise, sustained, and relaxation phases of visuomotor behavior were associated with clinically rated neuromotor issues in premutation carriers, indicating that select precision measures of visuomotor behavior may covary with FXTAS risk or progression.

**Reaction Time Slowing in Aging *FMR1* Premutation Carriers**

We observed increased reaction time in premutation carriers relative to healthy controls, and this effect was more severe at younger ages during rapid motor action (pulse task). Delayed reaction times in premutation carriers could reflect slowing of initial visual processing, delays in "premotor time" during which individuals translate sensory cues into a motor command, or slowing of the motor command and execution (Stelmach & Worringham, 1988). Based on the

specificity of premutation carriers' reaction time delays to the pulse task in which they had less preparatory time than sustained test conditions (2 vs. 8 sec), our findings implicate delays in premotor time or slowing of the motor command and execution. During a rapid motor task, relative to the sustained task, individuals have little time after a trial to prepare for the onset of the subsequent trial. During this premotor phase, individuals must prepare both an accurate and timely motor response, while flexibly shifting between gripping and relaxation. However, we observed increased reaction time independent of force level suggesting that delays in reaction time are not attributable to a slowed rate of actively engaging and increasing the firing rates of motor units but instead reflect delays in planning rapid actions.

Elevated reaction times in premutation carriers also were specific to younger premutation carriers among our aging adult sample, suggesting premutation carriers show degeneration of premotor response processes earlier than controls, but that overall levels of deterioration are similar by ages 60-70 years. It is important to note that none of the premutation carriers studied here self-reported clinical concerns of FXTAS, and our clinical data confirmed that premutation carriers in this study demonstrated reduced symptoms relative to FXTAS samples previously characterized using the ICARS (Berry-Kravis et al., 2003; Loesch, Churchyard, Brotchie, Marot, & Tassone, 2005). In the context of prior results indicating that the mean age of onset of FXTAS is 61 years (Tassone et al., 2007), our finding that delayed reaction times in premutation carriers are specific to ages 44-60 years suggests that alterations of motor planning processes may be specific to aging individuals who are still more susceptible to FXTAS. In contrast, elderly premutation carriers who have not experienced significant clinical deterioration prior to this age may show normative rates of reaction time slowing as they advance in age. Longitudinal studies will be needed to determine the extent to which slowed reactions times during rapid motor

actions may serve as prodromal markers of FXTAS for premutation carriers across aging and into elderly years.

**Rapid Force Production in *FMR1* Carriers**

Reduced rates of force increase and increased time to reach target force levels in aging premutation carriers together suggest impairment in the ability to rapidly increase force output during precision motor actions. These findings are not attributable to diminished overall force output as groups did not differ on MVC, and the overall amount of individuals' force generation was controlled in our analyses. Instead, premutation carriers appear to have a reduced ability to rapidly generate force, suggesting that the bradykinesia associated with FXTAS (Niu et al., 2014) may be evident in some asymptomatic premutation carriers. Similar reductions in initial force production also have been reported in studies of Parkinson's disease suggesting basal ganglia circuit functions may be affected during aging in premutation carriers (Fellows, Noth, & Schwarz, 1998; Stelmach & Worringham, 1988). This hypothesis is supported by studies highlighting increased iron deposition in neuronal and glial cells in putamen nuclei of FXTAS patients (Ariza et al., 2017) and case studies documenting pre- and postsynaptic nigrostriatal dysfunction (Healy et al., 2009; Scaglione et al., 2008; Zuhlke et al., 2004). Our findings also could reflect peripheral alterations. Although premutation carriers demonstrated similar MVCs compared to controls, atypical recruitment of motor neurons during voluntary muscle contractions is possible (Park et al., 2019; Rose & McGill, 2005; Wang et al., 2017). For example, a previous study has documented slower nerve conduction velocities and F-wave latencies in male premutation carriers with and without FXTAS (Soontarapornchai et al., 2008). EMG abnormalities, including reduced motor unit firing rates, have been reported in premutation carriers and FXTAS patients, indicating that difficulties generating force stem from alterations at

the neuromuscular level (Bravo et al., 2018; Lechpammer et al., 2017; Park et al., 2019). Both functional neuroimaging and EMG studies are needed to clarify mechanisms contributing to atypical rapid force production in premutation carriers.

At lower force levels (i.e., 15% and 45% MVC), premutation carriers showed a pattern of target overshooting compared to healthy controls. Movement dysmetria has been reported in several FXTAS case studies (Hagerman et al., 2004; Hall, Fraint, & Dafer, 2018), and our results add to these data suggesting that difficulties in feedforward motor planning also are present in asymptomatic aging premutation carriers. Whereas premutation carriers showed relatively intact abilities to produce accurate initial motor output at high force levels, their selective difficulties in overshooting low target force levels suggests reduced precision during more challenging fine motor tasks. Transient overshooting reflects imprecision in initial motor plans that is rapidly corrected in response to sensory feedback as seen at higher force levels that take longer to reach. This disproportionate impairment in the ability to plan fine motor behavior may have significant clinical consequences during activities of daily living, such as handwriting, as reported in prior case studies (Hagerman et al., 2012). Our finding that greater overshooting in premutation carriers was more prominent in the non-dominant relative to dominant hand suggests that feedforward motor deficits may have less impact initially during more skilled actions (e.g., those completed by the dominant hand). Given that our groups were matched on handedness, however, it is not likely that neurodegenerative processes affecting aging *FMR1* premutation carriers selectively compromise the right or left hemisphere.

**Sustained Visuomotor Control in *FMR1* Premutation Carriers**

During sustained force contractions, *FMR1* premutation carriers showed lower time series complexity (reduced ApEn) reflecting a reduced ability to dynamically adjust force output

in response to sensory feedback. Increased complexity of force output is adaptive and reflects individuals' ability to integrate multiple sensory feedback and feedforward processes and update their internal action model. Reduced complexity suggests reduced integration of these distinct processes and reduced ability to optimize precise sensorimotor behavior. Our finding that the severity of reduced sensory feedback control of force behavior in premutation carriers is relatively similar in magnitude across ages for the non-dominant hand, but more prominent at younger ages for the dominant hand indicates that deterioration of sustained sensorimotor motor behavior may be lateralized in aging premutation carriers. More specifically, our results suggest that healthy controls show worsening of their sustained force control as they age, whereas the opposite pattern is true for premutation carriers when using the dominant hand. We postulate that older premutation carriers in our sample who currently report being asymptomatic may be less affected by the premutation, and less likely to develop FXTAS than the younger individuals in our sample who are beginning to age into the period of adulthood during which they are most likely to develop FXTAS symptoms. This hypothesis is supported by evidence that FXTAS prevalence decreases during late adulthood reflecting increased FXTAS-related mortality rates and reduced likelihood of FXTAS onset during elderly years (Rodriguez-Revenga et al., 2009). Greater complexity for dominant compared to non-dominant hand performance in younger healthy controls likely accounts for the lateralized pattern of deficit seen in premutation carriers who showed similar levels of force complexity across hands.

Reduced complexity of the time-dependent structure of force oscillations in younger premutation carriers may reflect a reduced number of neural oscillators, as has been suggested by prior studies documenting reduced movement complexity in Parkinson's disease (Vaillancourt et al., 2001b). Neural oscillators within the central nervous system each generate rhythmic output.

Corticomotor neurons demonstrate preferred discharge frequencies, and so the use of a larger number of neural oscillators to generate motor output would result in greater complexity of motor output as each neural oscillator contributes output of a different frequency (McAuley & Marsden, 2000). Likewise, fewer neural oscillators generating motor output would result in the reduced variability of motor output timing consistent with a less complex and more rhythmic force output (McAuley & Marsden, 2000; Vaillancourt et al., 2001b). Our findings of reduced ApEn in premutation carriers thus implicate atypical integration of neural oscillators that may contribute to increased rates of tremor in premutation carriers (Homberg, Hefter, Reiners, & Freund, 1987). ApEn measurements during sustained visuomotor behavior hold promise for determining mechanisms contributing to tremor in FXTAS, and as surrogate biomarkers useful for clinical trials targeting tremor in patients (Hagerman et al., 2012).

In addition to reduced complexity of their sustained force output, premutation carriers also showed reduced sustained mean force output indicating motor dysmetria during feedback-guided visuomotor behavior. Reduced mean force may reflect peripheral weakness of neuromuscular processes in premutation carriers, though similar MVCs among premutation carriers and controls suggest motor weakness is not likely responsible for differences in mean force. Instead, mean force reductions likely indicate failures in sensory feedback guided motor behavior precision, consistent with a recent study documenting greater sustained force variability during finger abduction (Park et al., 2019). While we did not find evidence for atypical variability in our premutation carrier sample, our correlational analyses indicated that force variability was associated with more severe FXTAS symptoms suggesting that sustained sensorimotor dysmetria may be present in aging premutation carriers who are showing or beginning to show disease-related clinical issues.

**Visuomotor Behavior and FXTAS**

In addition to identifying multiple visuomotor behavioral alterations in aging premutation carriers, we also document strong relationships between visuomotor behavior and clinical symptoms of FXTAS. We found that increased reaction time, increased force variability, and faster rates of force relaxation each were associated with more severe clinically rated neuromotor issues in carriers suggesting that quantifiable deficits in multiple precision visuomotor behaviors may be part of the aging process in *FMR1* premutation carriers, or that these issues may reflect early indicators of atypical neurodegeneration associated with FXTAS. Our findings that delays in motor preparation processes are present primarily at earlier ages for our sample suggest that some premutation carriers may not show this deterioration. Instead, slower reaction times may reflect early indicators of FXTAS disease risk or progression. Alternatively, aging premutation carriers may show earlier decay of initial motor preparation and planning processes relative to healthy aging, but their rate of decay may slow and normalize with age. Our finding that greater force variability is associated with more severe FXTAS symptoms in premutation carriers indicates that a reduced ability to precisely and consistently maintain a steady motor output in response to sensory feedback information may track with developing symptoms in premutation carriers. Increased sustained force variability also is consistent with known neuropathological indicators of FXTAS. As individuals sustain a constant level of force using visual feedback, visual input typically is translated into motor corrections through parietal-ponto-cerebellar pathways. The MCP serves as the primary process relaying parietal-ponto visual feedback information to cerebellum, where motor corrections are translated. Degeneration of the MCP, reflected as hyperintensities on T2-weighted scans, is symptomatic of FXTAS and may

contribute to both greater sensorimotor variability and FXTAS clinical symptoms (Jacquemont et al., 2003).

Based on prior studies showing that greater CGG repeat length among premutation carriers increases risk for FXTAS (Tassone et al., 2007), our finding that reduced ApEn was related to increased CGG repeat length in premutation carriers also suggests that sustained visuomotor behavioral issues may covary with disease risk. From a more mechanistic perspective, greater CGG repeat length in the premutation range contributes to increased mRNA transcript, sequestration of proteins, and intranuclear inclusions (Greco et al., 2006; Li & Jin, 2012). These inclusions have been documented in pontine and cerebellar cells in the majority of cases studied to date (Ariza et al., 2016; Greco et al., 2006), suggesting that greater CGG repeat length compromises ponto-cerebellar functions. The atypical sensorimotor behaviors identified in this study are consistent with this model and may serve as objective biobehavioral targets useful for understanding pathophysiological processes associated with FXTAS and quantifying clinically relevant changes in aging premutation carriers.

**Limitations**

Several limitations of the present study should be acknowledged. First, larger samples of FXTAS patients and asymptomatic premutation carriers are needed to examine variability in visuomotor behavior during aging and determine disease-specific markers. Longitudinal samples are needed to track disease onset and progression and clarify the extent to which objective measures of visuomotor precision may track with disease course. Second, it will be critical to include movement disorder comparison groups in future studies of aging premutation carriers to determine the specificity of these metrics to this population, though we propose that the next critical step is to determine the specificity of key visuomotor issues to symptomatic compared to

asymptomatic *FMR1* premutation carriers so that disease presence can be reliably identified in aging individuals who test positive for premutation alleles. Third, our sample consisted primarily of females who are at reduced risk for FXTAS relative to males. Despite 75% of our sample being female, we established multiple visuomotor issues in aging premutation carriers and identified multiple participants, both male and female, showing FXTAS symptoms. Inclusion of females in FXTAS studies is warranted, though larger samples that allow for direct comparisons of sensorimotor behavior in aging males and females are needed. Fourth, while we report behavioral findings in relation to CGG repeat length, measures of mRNA, methylation ratios, and FMR protein are important for clarifying how aberrant neurobiological processes contribute to FXTAS risk or prodromal symptoms.

## Conclusions

Our results identify multiple precision visuomotor issues in aging *FMR1* premutation carriers and indicate that select visuomotor alterations track with FXTAS symptom severity. Together, these findings suggest that subclinical deficits of precision visuomotor behavior may be detectable prior to the onset of FXTAS and serve as key targets for tracking disease risk and monitoring disease progression.

Table 1

*Demographic and Clinical Characteristics for Healthy Controls and FMR1 Premutation Carriers*

| | **Controls** (*n* = 31) | **Premutation Carriers** (*n* = 26) | ***t*** | ***p*** |
|---|---|---|---|---|
| Age (years) | 53.29 (9.79) | 56.77 (8.87) | -1.39 | .169 |
| Sex (% male) † | 38.7% | 23.1% | 1.60† | .206 |
| Handedness (% right) † | 90.3% | 96.2% | .737† | .391 |
| FSIQ | 109.32 (12.83) | 99.48 (12.07) | **2.93** | **.005**** |
| ICARS total score | - | 5.47 (4.76) | - | - |
| ICARS total range | - | 0-19 | - | - |
| CGG repeat length | - | 82 (17) | - | - |

*Note*: FSIQ: full-scale IQ; ICARS: International Cooperative Ataxia Rating Scale; CGG: cytosine-guanine-guanine. Variables are presented as: mean (standard deviation); **p < .01; †chi-square statistic

Table 2

*Best Fitting Multilevel Models for Reaction Time and Rise Phase Rate of Force Increase*

| | **Fixed Effect Estimates** | | ***p*** | **Random Effect Variances** | |
|---|---|---|---|---|---|
| **Rise phase latency** | Level 1 Variables | | | Level 1 residual ($\varepsilon_{it}$) | 0.020 (0.142) |
| | Intercept | 0.456 (0.022) | < .001 | Level 2 intercept ($\mu_{0i}$) | 0.025 (0.158) |
| | % MVC | 0.072 (0.014) | < .001 | | |
| | Task | 0.086 (0.012) | < .001 | | |
| | Level 2 Variables | | | | |
| | Group | 0.026 (0.045) | .557 | | |
| | Age | 0.049 (0.023) | .034 | | |
| | Interaction Variables | | | | |
| | Group x Age | -0.012 (0.045) | .799 | | |
| | Group x Task | -0.014 (0.024) | .575 | | |
| | Task x Age | -0.023 (0.014) | .102 | | |
| | Group x Age x Task | -0.099 (0.028) | < .001 | | |
| | **Fixed Effect Estimates** | | ***p*** | **Random Effect Variances** | |
| **Rate of force increase** | Level 1 Variables | | | Level 1 residual ($\varepsilon_{it}$) | 0.288 (0.537) |
| | Intercept | 1.894 (0.060) | < .001 | Level 2 intercept ($\mu_{0i}$) | 0.169 (0.411) |
| | % MVC | 1.987 (0.082) | < .001 | % MVC | 0.205 (0.453) |
| | Hand | 0.201 (0.044) | < .001 | | |
| | Task | -0.386 (0.046) | < .001 | | |
| | Level 2 Variables | | | | |
| | Group | -0.158 (0.120) | .196 | | |
| | Age | -0.051 (0.062) | .409 | | |
| | Interaction Variables | | | | |
| | Group x % MVC | -0.221 (0.164) | .182 | | |
| | Group x Age | 0.335 (0.124) | .009 | | |
| | Group x Task | 0.268 (0.091) | .004 | | |
| | % MVC x Age | -0.032 (0.085) | .707 | | |
| | % MVC x Task | -0.616 (0.109) | < .001 | | |
| | Task x Age | -0.112 (0.052) | .031 | | |
| | Group x % MVC x Age | 0.339 (0.169) | .049 | | |
| | Group x % MVC x Task | 0.625 (0.217) | .004 | | |
| | Group x Age x Task | -0.316 (0.104) | .002 | | |

*Note*: MVC: maximum voluntary contraction; Fixed effect estimate values are given as Estimate (Standard Error) and random effect variances are given as Variance (Standard Deviation); rate of force increase controls for participant MVC

Table 3

*Best Fitting Multilevel Models for Rise Phase Duration and Accuracy*

| | **Fixed Effect Estimates** | | ***p*** | **Random Effect Variances** | |
|---|---|---|---|---|---|
| **Rise phase duration** | Level 1 Variables | | | Level 1 residual ($\varepsilon_{it}$) | 0.00001 (0.004) |
| | Intercept | 0.014 (0.001) | < .001 | Level 2 intercept ($\mu_{0i}$) | 0.00002 (0.005) |
| | % MVC | 0.001 (0.0004) | .003 | | |
| | Hand | -0.0001 (0.0003) | .697 | | |
| | Task | -0.004 (0.0003) | < .001 | | |
| | Level 2 Variables | | | | |
| | Group | 0.0005 (0.001) | .714 | | |
| | Age | -0.0003 (0.0007) | .698 | | |
| | Interaction Variables | | | | |
| | Group x Hand | -0.002 (0.0006) | .002 | | |
| | Task x Age | 0.0009 (0.0004) | .015 | | |
| | **Fixed Effect Estimates** | | ***p*** | **Random Effect Variances** | |
| **Rise phase accuracy** | Level 1 Variables | | | Level 1 residual ($\varepsilon_{it}$) | 0.002 (0.049) |
| | Intercept | 0.998 (0.003) | < .001 | Level 2 intercept ($\mu_{0i}$) | 0.0004 (0.020) |
| | % MVC | -0.075 (0.008) | < .001 | % MVC | 0.002 (0.049) |
| | Hand | 0.005 (0.004) | .217 | | |
| | Task | -0.015 (0.004) | < .001 | | |
| | Level 2 Variables | | | | |
| | Group | 0.009 (0.007) | .192 | | |
| | Interaction Variables | | | | |
| | Hand x % MVC | -0.009 (0.010) | 0.386 | | |
| | Group x % MVC | -0.014 (0.016) | 0.362 | | |
| | Group x Hand | 0.005 (0.008) | 0.540 | | |
| | Task x Hand | -0.002 (0.008) | 0.809 | | |
| | Group x Task | -0.006 (0.008) | 0.477 | | |
| | Group x % MVC x Hand | -0.047 (0.020) | 0.017 | | |
| | Group x Task x Hand | -0.033 (0.016) | 0.044 | | |

*Note*: MVC: maximum voluntary contraction; Fixed effect estimate values are given as Estimate (Standard Error) and random effect variances are given as Variance (Standard Deviation); rise phase duration controls for participant MVC

Table 4

*Best Fitting Multilevel Models for Sustained Phase Variables*

| | **Fixed Effect Estimates** | | ***p*** | **Random Effect Variances** | |
|---|---|---|---|---|---|
| **ApEn** | Level 1 Variables | | | Level 1 residual ($\varepsilon_{it}$) | 0.006 (0.074) |
| | Intercept | 0.428 (0.009) | < .001 | Level 2 intercept ($\mu_{0i}$) | 0.003 (0.059) |
| | % MVC | -0.124 (0.014) | < .001 | % MVC | 0.005 (0.077) |
| | Hand | -0.013 (0.008) | .108 | | |
| | Level 2 Variables | | | | |
| | Group | -0.029 (0.017) | .094 | | |
| | Age | 0.011 (0.009) | .227 | | |
| | Interaction Variables | | | | |
| | Group x Hand x Age | -0.041 (0.017) | .014 | | |
| | Group x Age | 0.020 (0.017) | .251 | | |
| | Group x Hand | -0.013 (0.016) | .431 | | |
| | Hand x Age | 0.006 (0.008) | .450 | | |
| | **Fixed Effect Estimates** | | ***p*** | **Random Effect Variances** | |
| **Force SD** | Level 1 Variables | | | Level 1 residual ($\varepsilon_{it}$) | 2.760 (1.661) |
| | Intercept | 1.673 (0.189) | < .001 | Level 2 intercept ($\mu_{0i}$) | 1.569 (1.253) |
| | % MVC | 3.348 (0.477) | < .001 | % MVC | 10.207 (3.195) |
| | Hand | 0.470 (0.180) | .010 | | |
| | **Fixed Effect Estimates** | | ***p*** | **Random Effect Variances** | |
| **Mean Force** | Level 1 Variables | | | Level 1 residual ($\varepsilon_{it}$) | 20.600 (4.538) |
| | Intercept | 38.850 (2.371) | < .001 | Level 2 intercept ($\mu_{0i}$) | 154.700 (12.439) |
| | % MVC | 54.478 (2.371) | < .001 | % MVC | 299.8 (17.316) |
| | Hand | 0.220 (0.494) | .657 | | |
| | Level 2 Variables | | | | |
| | Group | 0.351 (0.976) | .719 | | |
| | Interaction Variables | | | | |
| | Group x Hand | 3.480 (0.988) | < .001 | | |

*Note*: MVC: maximum voluntary contraction; Fixed effect estimate values are given as Estimate (Standard Error) and random effect variances are given as Variance (Standard Deviation)

Table 5

*Correlational Analyses of CGG and Visuomotor Outcomes (Spearman ρ Values)*

| | | 2-second ("Pulse") | | | 8-second ("Sustained") | | |
|---|---|---|---|---|---|---|---|
| | | MVC Level | | | MVC Level | | |
| | **Dependent Variable** | **15%** | **45%** | **85%** | **15%** | **45%** | **85%** |
| **Dominant Hand** | Rise phase accuracy | -0.209 | -0.144 | -0.379 | 0.024 | -0.046 | -0.010 |
| | Rate of force increase | 0.032 | -0.151 | 0.277 | -0.151 | 0.277 | 0.033 |
| | Rise phase duration | 0.193 | 0.015 | 0.169 | 0.015 | 0.169 | 0.137 |
| | Rise phase latency | 0.525* | 0.437* | 0.345 | 0.437* | 0.345 | 0.124 |
| | Mean force | - | - | - | -0.107 | -0.128 | -0.155 |
| | ApEn | - | - | - | -0.330 | **-0.529**** | -0.453* |
| | Force SD | - | - | - | 0.222 | 0.191 | 0.320 |
| | Rate of force relaxation | -0.255 | -0.272 | -0.068 | -0.272 | -0.068 | 0.122 |
| | **Dependent Variable** | **15%** | **45%** | **85%** | **15%** | **45%** | **85%** |
| **Non-Dominant Hand** | Rise phase accuracy | -0.209 | -0.144 | -0.379 | 0.286 | 0.266 | -0.246 |
| | Rate of force increase | 0.110 | 0.045 | 0.039 | 0.045 | 0.039 | -0.195 |
| | Rise phase duration | 0.221 | 0.417* | 0.200 | 0.417* | 0.200 | 0.374 |
| | Rise phase latency | 0.214 | 0.457* | 0.296 | 0.457* | 0.296 | 0.355 |
| | Mean force | - | - | - | -0.085 | -0.103 | -0.067 |
| | ApEn | - | - | - | -0.388 | -0.449* | -0.382 |
| | Force SD | - | - | - | 0.348 | 0.183 | 0.081 |
| | Rate of force relaxation | 0.056 | -0.102 | -0.008 | -0.102 | -0.008 | -0.174 |

*Note*: MVC: maximum voluntary contraction; CGG: cytosine-guanine-guanine; *$p < .05$**; **$p < .01$;**
Rates of force relaxation are negative values, and so positive correlations indicate that an increase in CGG repeat length is associated with slower (i.e., less negative) rates of force relaxation.

Table 6

*Correlational Analyses of Total ICARS Scores and Visuomotor Outcomes (Spearman ρ Values)*

| | | 2-second ("Pulse") | | | 8-second ("Sustained") | | |
|---|---|---|---|---|---|---|---|
| | | MVC Level | | | MVC Level | | |
| | **Dependent Variable** | **15%** | **45%** | **85%** | **15%** | **45%** | **85%** |
| **Dominant Hand** | Rise phase accuracy | -0.343 | 0.081 | -0.057 | -0.112 | 0.121 | -0.423 |
| | Rate of force increase | 0.519 | 0.459 | 0.470 | -0.182 | -0.117 | 0.053 |
| | Rise phase duration | -0.353 | -0.421 | -0.124 | -0.270 | -0.022 | 0.068 |
| | Rise phase latency | **0.774**** | 0.703* | **0.724**** | **0.612**** | 0.182 | 0.336 |
| | Mean force | - | - | - | 0.139 | 0.083 | 0.085 |
| | ApEn | - | - | - | -0.178 | 0.022 | -0.195 |
| | Force SD | - | - | - | 0.223 | 0.401 | 0.414 |
| | Rate of force relaxation | **-0.827**** | **-0.841**** | -0.636* | -0.273 | -0.163 | -0.095 |
| | **Dependent Variable** | **15%** | **45%** | **85%** | **15%** | **45%** | **85%** |
| **Non-Dominant Hand** | Rise phase accuracy | -0.343 | 0.081 | -0.057 | -0.035 | 0.216 | -0.427 |
| | Rate of force increase | 0.194 | 0.336 | 0.208 | -0.305 | 0.012 | -0.227 |
| | Rise phase duration | -0.371 | -0.389 | -0.424 | -0.018 | 0.200 | 0.005 |
| | Rise phase latency | 0.551 | 0.625* | **0.795**** | 0.372 | 0.441 | 0.248 |
| | Mean force | - | - | - | 0.092 | 0.143 | 0.113 |
| | ApEn | - | - | - | -0.395 | -0.173 | -0.377 |
| | Force SD | - | - | - | 0.339 | **0.663**** | 0.578* |
| | Rate of force relaxation | -0.463 | -0.399 | -0.219 | 0.121 | -0.014 | 0.383 |

*Note*: MVC: maximum voluntary contraction; CGG: cytosine-guanine-guanine; *$p < .05$**; **$p < .01$;**
Rates of force relaxation are negative values, and so positive correlations indicate that an increase in CGG repeat length is associated with slower (i.e., less negative) rates of force relaxation.

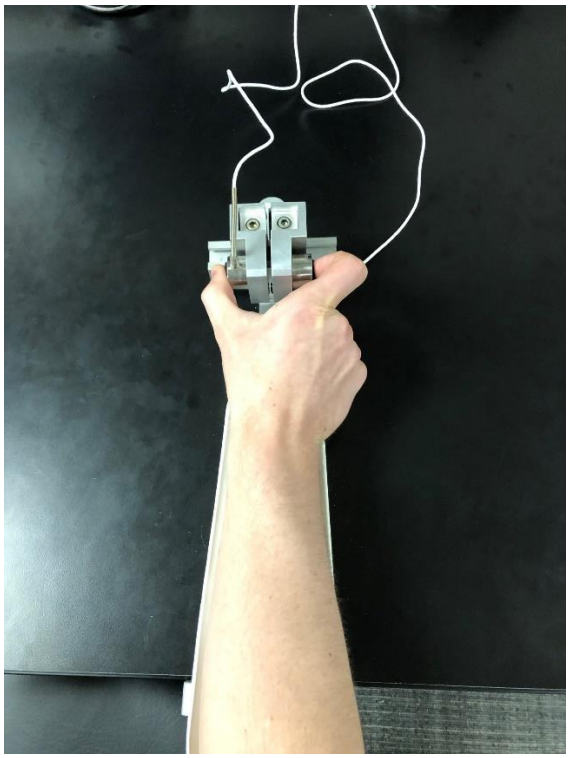

*Figure 1*: The custom-made arm brace and load cells for laboratory testing. Participants pressed with their thumb and forefinger against two precision load cells while viewing two horizontal bars displayed vertically on the screen.

*Figure 2*: Visuomotor test stimuli. Participants pressed when the red bar turned green in order to bring the white bar up to the target green bar. They were instructed to maintain their force level at the level of the green bar as steadily as possible.

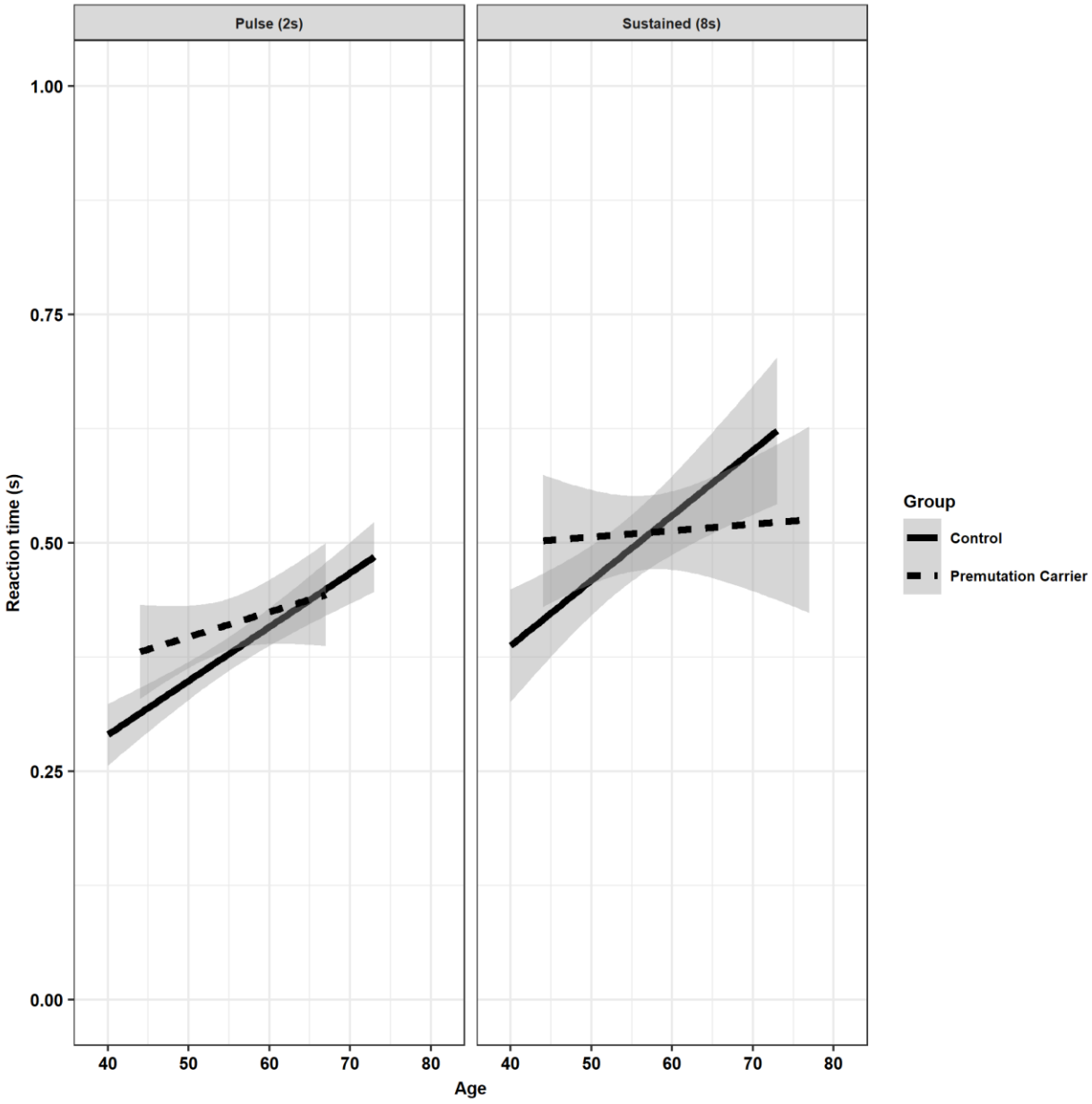


*Figure 3*: Rise phase reaction time as a function of group, task, and age (linear fit with 95% confidence intervals). Relative to controls, premutation carriers demonstrate longer reaction times during the pulse task at younger ages. At older ages, premutation carriers show similar reaction times to controls during the pulse task. During the sustained task, premutation carriers, regardless of age, show similar reaction times, whereas older controls perform more slowly with age.

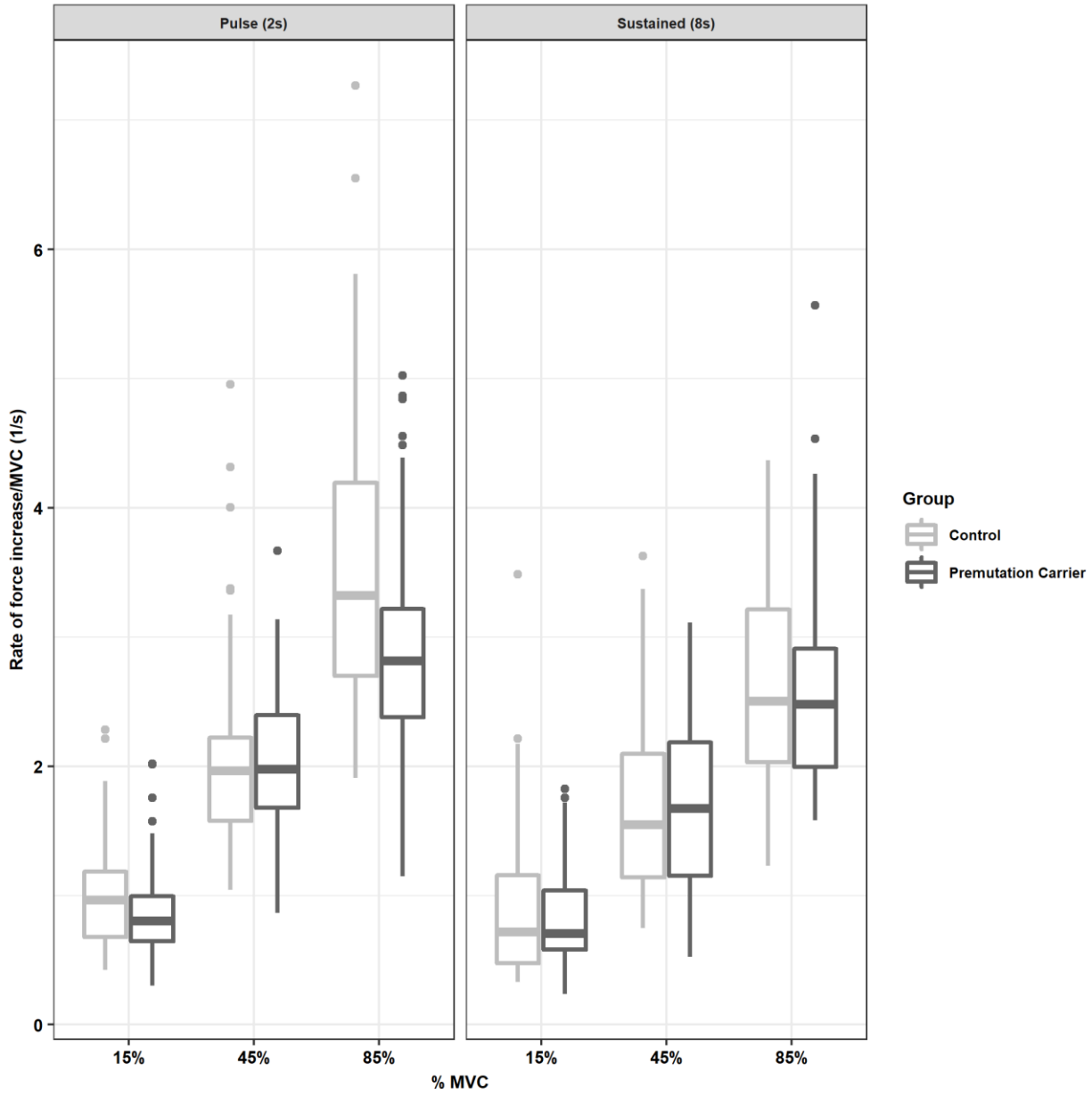


*Figure 4*: Peak rate of force increase (controlled for individual MVC) as a function of group, task, and % MVC. Relative to controls, premutation carriers show a reduced rate of force increase during the 85% MVC pulse task. Lower and upper box bounds represent the 25$^{th}$ and 75$^{th}$ percentiles, respectively. Upper and lower whiskers extend at most to 1.5 times the interquartile range.

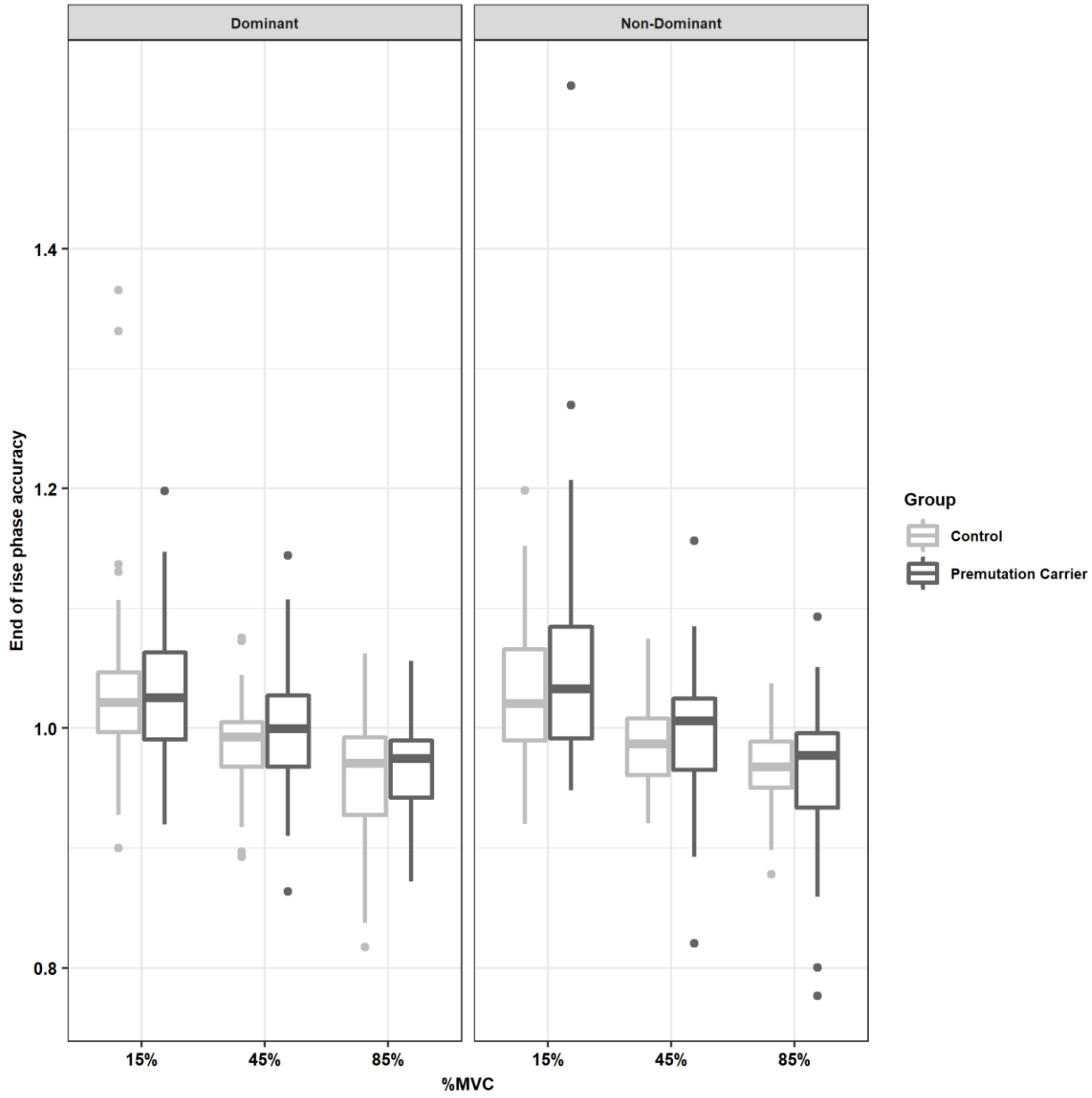


*Figure 5*: Rise phase accuracy as a function of group, hand, and % MVC. A value of 1 reflects perfect accuracy. Relative to controls, premutation carriers overshoot target force levels when using their non-dominant hand in low force conditions (15% and 45%). Lower and upper box bounds represent the 25$^{th}$ and 75$^{th}$ percentiles, respectively. Upper and lower whiskers extend at most to 1.5 times the interquartile range.

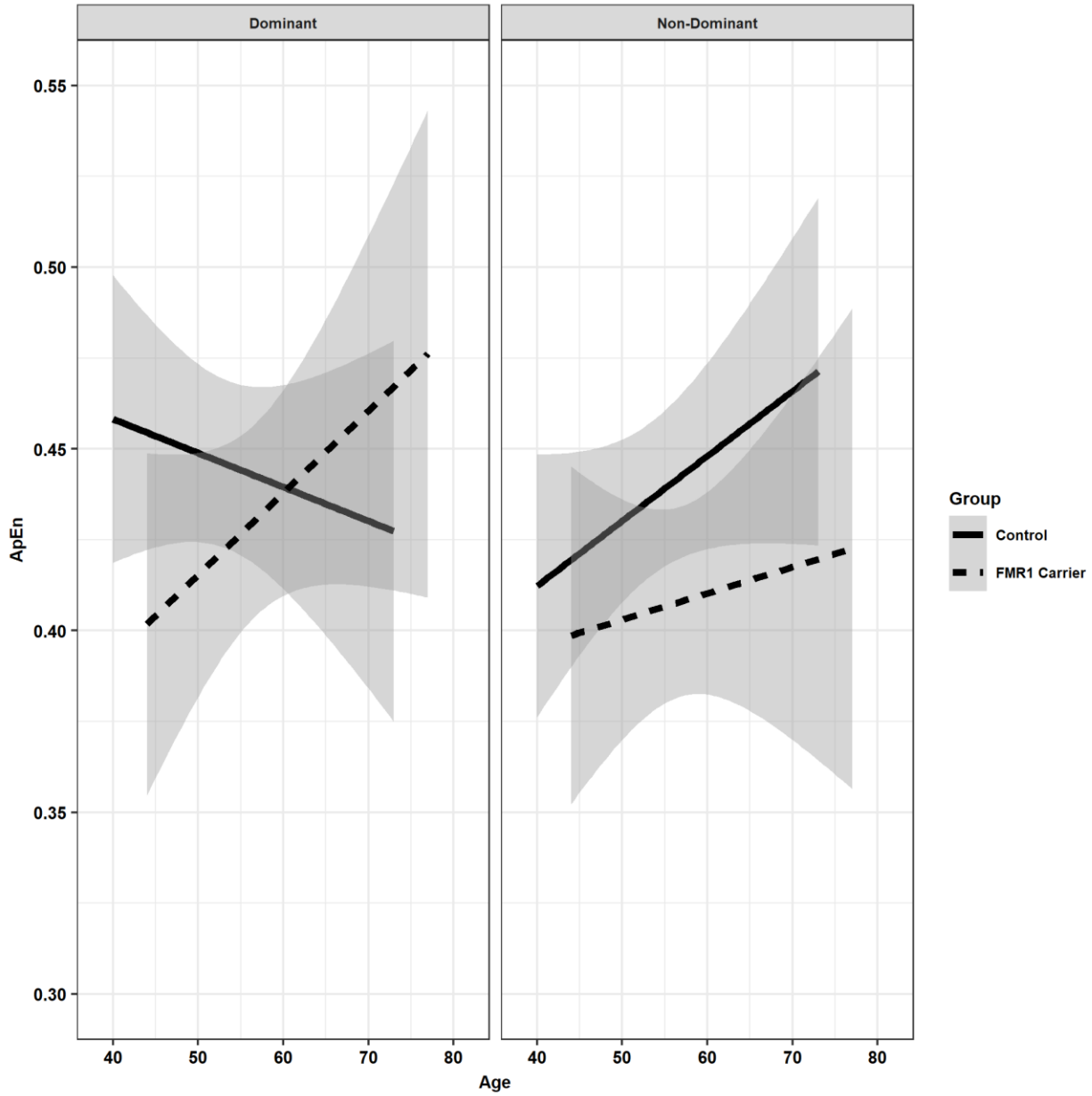


*Figure 6*: Approximate entropy (ApEn; i.e., force complexity) as a function of group, hand, and age (linear fit with 95% confidence intervals). During the dominant hand condition, younger premutation carriers demonstrated reduced force complexity, while premutation carriers across a broad age range demonstrated reduced force complexity during the non-dominant hand condition.

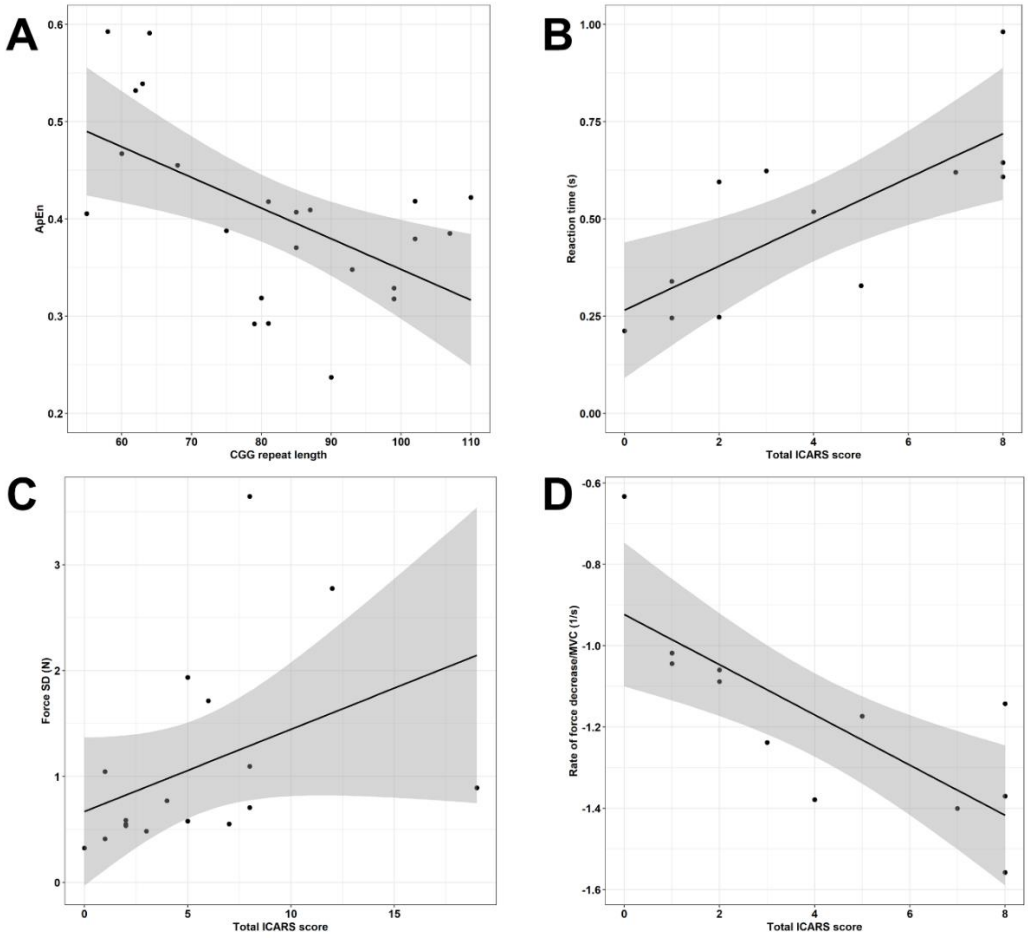


*Figure 7:* A. CGG (cytosine-guanine-guanine) repeat length is associated with reduced non-dominant hand approximate entropy (ApEn), a measure of the complexity of force output, during the 45% MVC condition. B. Increased total ICARS scores (clinical severity) are associated with longer reaction time across multiple conditions (non-dominant, 85% MVC, pulse task is shown as a representative relationship). C. Increased total ICARS scores (clinical severity) are associated with increased force variability (force SD) during the non-dominant hand 45% MVC condition. D. Increased total ICARS scores (clinical severity) are associated with more negative (i.e., quicker) rates of force relaxation during multiple conditions (dominant, 15% MVC, pulse task is shown as a representative relationship). All shaded error bars represent the 95% confidence of a linear fit.

## References


Aguilar, D., Sigford, K. E., Soontarapornchai, K., Nguyen, D. V., Adams, P. E., Yuhas, J. M., . . . Hagerman, R. J. (2008). A quantitative assessment of tremor and ataxia in FMR1 premutation carriers using CATSYS. *American Journal of Medical Genetics. Part A, 146A*(5), 629-635. Retrieved from https://www.ncbi.nlm.nih.gov/pubmed/18241072. doi:10.1002/ajmg.a.32211

Ariza, J., Rogers, H., Hartvigsen, A., Snell, M., Dill, M., Judd, D., . . . Martinez-Cerdeno, V. (2017). Iron accumulation and dysregulation in the putamen in fragile X-associated tremor/ataxia syndrome. *Movement Disorders, 32*(4), 585-591. Retrieved from https://www.ncbi.nlm.nih.gov/pubmed/28233916. doi:10.1002/mds.26902

Ariza, J., Rogers, H., Monterrubio, A., Reyes-Miranda, A., Hagerman, P. J., & Martinez-Cerdeno, V. (2016). A majority of FXTAS cases present with intranuclear inclusions within Purkinje cells. *Cerebellum, 15*(5), 546-551. Retrieved from https://www.ncbi.nlm.nih.gov/pubmed/27108270. doi:10.1007/s12311-016-0776-y

Berry-Kravis, E., Lewin, F., Wuu, J., Leehey, M., Hagerman, R., Hagerman, P., & Goetz, C. G. (2003). Tremor and ataxia in fragile X premutation carriers: blinded videotape study. *Annals of Neurology, 53*(5), 616-623. Retrieved from https://www.ncbi.nlm.nih.gov/pubmed/12730995. doi:10.1002/ana.10522

Bravo, G. A., Fernandez-Carril, J. M., Lopez-Zuazo, I., Izquierdo, A. Y., Abrol, T., & Alsinaidi, O. (2018). A novel clinical phenotype of fragile X-associated tremor/ataxia syndrome. *Movement Disorders Clinical Practice, 5*(4), 430-432. Retrieved from WOS:000442220200012. doi:10.1002/mdc3.12637

Brunberg, J. A., Jacquemont, S., Hagerman, R. J., Berry-Kravis, E. M., Grigsby, J., Leehey, M. A., . . . Hagerman, P. J. (2002). Fragile X premutation carriers: characteristic MR imaging findings of adult male patients with progressive cerebellar and cognitive dysfunction. *AJNR: American Journal of Neuroradiology, 23*(10), 1757-1766. Retrieved from https://www.ncbi.nlm.nih.gov/pubmed/12427636.

Chu, W. T., & Sanger, T. D. (2009). Force variability during isometric biceps contraction in children with secondary dystonia due to cerebral palsy. *Movement Disorders, 24*(9), 1299-1305. Retrieved from https://www.ncbi.nlm.nih.gov/pubmed/19412940. doi:10.1002/mds.22573

Desmurget, M., Epstein, C. M., Turner, R. S., Prablanc, C., Alexander, G. E., & Grafton, S. T. (1999). Role of the posterior parietal cortex in updating reaching movements to a visual target. *Nature Neuroscience, 2*(6), 563-567. Retrieved from https://www.ncbi.nlm.nih.gov/pubmed/10448222. doi:10.1038/9219

Ehrsson, H. H., Fagergren, A., Jonsson, T., Westling, G., Johansson, R. S., & Forssberg, H. (2000). Cortical activity in precision- versus power-grip tasks: an fMRI study. *Journal of Neurophysiology, 83*(1), 528-536. Retrieved from https://www.ncbi.nlm.nih.gov/pubmed/10634893. doi:10.1152/jn.2000.83.1.528

Fellows, S. J., Noth, J., & Schwarz, M. (1998). Precision grip and Parkinson's disease. *Brain, 121 ( Pt 9)*, 1771-1784. Retrieved from https://www.ncbi.nlm.nih.gov/pubmed/9762964. doi:doi: 10.1093/brain/121.9.1771

Ghez, C., Hening, W., & Gordon, J. (1991). Organization of voluntary movement. *Current Opinion in Neurobiology, 1*(4), 664-671. Retrieved from https://www.ncbi.nlm.nih.gov/pubmed/1822314. doi:10.1016/S0959-4388(05)80046-7

Grafton, S. T., & Tunik, E. (2011). Human basal ganglia and the dynamic control of force during on-line corrections. *Journal of Neuroscience, 31*(5), 1600-1605. Retrieved from WOS:000286922100007. doi:10.1523/Jneurosci.3301-10.2011

Greco, C. M., Berman, R. F., Martin, R. M., Tassone, F., Schwartz, P. H., Chang, A., . . . Hagerman, P. J. (2006). Neuropathology of fragile X-associated tremor/ataxia syndrome (FXTAS). *Brain, 129*(Pt 1), 243-255. Retrieved from https://www.ncbi.nlm.nih.gov/pubmed/16332642. doi:10.1093/brain/awh683

Grigsby, J., Brega, A. G., Engle, K., Leehey, M. A., Hagerman, R. J., Tassone, F., . . . Reynolds, A. (2008). Cognitive profile of fragile X premutation carriers with and without fragile X-associated tremor/ataxia syndrome. *Neuropsychology, 22*(1), 48-60. Retrieved from https://www.ncbi.nlm.nih.gov/pubmed/18211155. doi:10.1037/0894-4105.22.1.48

Hagerman, R. J., Leavitt, B. R., Farzin, F., Jacquemont, S., Greco, C. M., Brunberg, J. A., . . . Hagerman, P. J. (2004). Fragile-X-associated tremor/ataxia syndrome (FXTAS) in females with the FMR1 premutation. *American Journal of Human Genetics, 74*(5), 1051-1056. Retrieved from https://www.ncbi.nlm.nih.gov/pubmed/15065016. doi:10.1086/420700

Hagerman, R. J., Leehey, M., Heinrichs, W., Tassone, F., Wilson, R., Hills, J., . . . Hagerman, P. J. (2001). Intention tremor, parkinsonism, and generalized brain atrophy in male carriers of fragile X. *Neurology, 57*(1), 127-130. Retrieved from https://www.ncbi.nlm.nih.gov/pubmed/11445641. doi:10.1212/WNL.57.1.127

Hagerman, R. J., Pak, J. S., Ortigas, M., Olichnew, J., Frysinger, R., Harrison, M., . . . Shahlaie, K. (2012). Case series: deep brain stimulation in patients with FXTAS. *Brain Disorders & Therapy, 1*(2). doi:10.4172/2168-975X.1000104

Hall, D. A., Fraint, A., & Dafer, R. (2018). Acute stroke in middle cerebellar peduncle in a patient with FXTAS. *Front Genet, 9*, 187. Retrieved from https://www.ncbi.nlm.nih.gov/pubmed/29887875. doi:10.3389/fgene.2018.00187

Healy, D. G., Bressman, S., Dickson, J., Silveira-Moriyama, L., Schneider, S. A., Sullivan, S. S., . . . Lees, A. J. (2009). Evidence for pre and postsynaptic nigrostriatal dysfunction in the fragile X tremor-ataxia syndrome. *Movement Disorders, 24*(8), 1245-1247. Retrieved from https://www.ncbi.nlm.nih.gov/pubmed/19260103. doi:10.1002/mds.22267

Homberg, V., Hefter, H., Reiners, K., & Freund, H. J. (1987). Differential effects of changes in mechanical limb properties on physiological and pathological tremor. *Journal of Neurology, Neurosurgery and Psychiatry, 50*(5), 568-579. Retrieved from https://www.ncbi.nlm.nih.gov/pubmed/3585382. doi:10.1136/jnnp.50.5.568

Jacquemont, S., Hagerman, R. J., Leehey, M., Grigsby, J., Zhang, L., Brunberg, J. A., . . . Hagerman, P. J. (2003). Fragile X premutation tremor/ataxia syndrome: Molecular, clinical, and neuroimaging correlates. *American Journal of Human Genetics, 72*(4), 869-878. Retrieved from WOS:000181972600008. doi:10.1086/374321

Jacquemont, S., Hagerman, R. J., Leehey, M. A., Hall, D. A., Levine, R. A., Brunberg, J. A., . . . Hagerman, P. J. (2004). Penetrance of the fragile X-associated tremor/ataxia syndrome in a premutation carrier population. *JAMA, 291*(4), 460-469. Retrieved from https://www.ncbi.nlm.nih.gov/pubmed/14747503. doi:10.1001/jama.291.4.460

Juncos, J. L., Lazarus, J. T., Graves-Allen, E., Shubeck, L., Rusin, M., Novak, G., . . . Sherman, S. L. (2011). New clinical findings in the fragile X-associated tremor ataxia syndrome (FXTAS). *Neurogenetics, 12*(2), 123-135. Retrieved from https://www.ncbi.nlm.nih.gov/pubmed/21279400. doi:10.1007/s10048-010-0270-5

Kraan, C. M., Hocking, D. R., Georgiou-Karistianis, N., Metcalfe, S. A., Archibald, A. D., Fielding, J., . . . Cornish, K. M. (2013). Cognitive-motor interference during postural control indicates at-risk cerebellar profiles in females with the FMR1 premutation. *Behavioural Brain Research, 253*, 329-336. Retrieved from https://www.ncbi.nlm.nih.gov/pubmed/23896050. doi:10.1016/j.bbr.2013.07.033

Kremer, E. J., Yu, S., Pritchard, M., Nagaraja, R., Heitz, D., Lynch, M., . . . et al. (1991). Isolation of a human DNA sequence which spans the fragile X. *American Journal of Human Genetics, 49*(3), 656-661. Retrieved from https://www.ncbi.nlm.nih.gov/pubmed/1882843.

Kuhtz-Buschbeck, J. P., Gilster, R., Wolff, S., Ulmer, S., Siebner, H., & Jansen, O. (2008). Brain activity is similar during precision and power gripping with light force: An fMRI study. *Neuroimage, 40*(4), 1469-1481. Retrieved from WOS:000255347100004. doi:10.1016/j.neuroimage.2008.01.037

Lechpammer, M., Cerdeno, V. M., Hunsaker, M. R., Hah, M., Gonzales, H., Tisch, S., . . . Hagerman, R. J. (2017). Concomitant occurrence of FXTAS and clinically defined sporadic inclusion body myositis: report of two cases. *Croatian Medical Journal, 58*(4), 310-315. Retrieved from WOS:000410623400007. doi:10.3325/cmj.2017.58.310

Leehey, M. A., Berry-Kravis, E., Min, S. J., Hall, D. A., Rice, C. D., Zhang, L., . . . Hagerman, P. J. (2007). Progression of tremor and ataxia in male carriers of the FMR1 premutation. *Movement Disorders, 22*(2), 203-206. Retrieved from https://www.ncbi.nlm.nih.gov/pubmed/17133502. doi:10.1002/mds.21252

Li, Y., & Jin, P. (2012). RNA-mediated neurodegeneration in fragile X-associated tremor/ataxia syndrome. *Brain Research, 1462*, 112-117. Retrieved from https://www.ncbi.nlm.nih.gov/pubmed/22459047. doi:10.1016/j.brainres.2012.02.057

Loesch, D. Z., Churchyard, A., Brotchie, P., Marot, M., & Tassone, F. (2005). Evidence for, and a spectrum of, neurological involvement in carriers of the fragile X pre-mutation: FXTAS and beyond. *Clinical Genetics, 67*(5), 412-417. Retrieved from https://www.ncbi.nlm.nih.gov/pubmed/15811008. doi:10.1111/j.1399-0004.2005.00425.x

Lozano, R., Rosero, C. A., & Hagerman, R. J. (2014). Fragile X spectrum disorders. *Intractable Rare Dis Res, 3*(4), 134-146. Retrieved from https://www.ncbi.nlm.nih.gov/pubmed/25606363. doi:10.5582/irdr.2014.01022

McAuley, J. H., & Marsden, C. D. (2000). Physiological and pathological tremors and rhythmic central motor control. *Brain, 123 ( Pt 8)*, 1545-1567. Retrieved from https://www.ncbi.nlm.nih.gov/pubmed/10908186. doi:10.1093/brain/123.8.1545

Mosconi, M. W., Mohanty, S., Greene, R. K., Cook, E. H., Vaillancourt, D. E., & Sweeney, J. A. (2015). Feedforward and feedback motor control abnormalities implicate cerebellar dysfunctions in autism spectrum disorder. *Journal of Neuroscience, 35*(5), 2015-2025. Retrieved from https://www.ncbi.nlm.nih.gov/pubmed/25653359. doi:10.1523/JNEUROSCI.2731-14.2015

Neely, K. A., Coombes, S. A., Planetta, P. J., & Vaillancourt, D. E. (2013). Segregated and overlapping neural circuits exist for the production of static and dynamic precision grip force. *Human Brain Mapping, 34*(3), 698-712. Retrieved from https://www.ncbi.nlm.nih.gov/pubmed/22109998. doi:10.1002/hbm.21467

Niu, Y. Q., Yang, J. C., Hall, D. A., Leehey, M. A., Tassone, F., Olichney, J. M., . . . Zhang, L. (2014). Parkinsonism in fragile X-associated tremor/ataxia syndrome (FXTAS): revisited.

*Parkinsonism & Related Disorders, 20*(4), 456-459. Retrieved from https://www.ncbi.nlm.nih.gov/pubmed/24491663. doi:10.1016/j.parkreldis.2014.01.006

O'Keefe, J. A., Robertson-Dick, E., Dunn, E. J., Li, Y., Deng, Y., Fiutko, A. N., . . . Hall, D. A. (2015). Characterization and early detection of balance deficits in fragile X premutation carriers with and without fragile X-associated tremor/ataxia syndrome (FXTAS). *Cerebellum, 14*(6), 650-662. Retrieved from https://www.ncbi.nlm.nih.gov/pubmed/25763861. doi:10.1007/s12311-015-0659-7

Park, S. H., Wang, Z., McKinney, W., Khemani, P., Lui, S., Christou, E. A., & Mosconi, M. W. (2019). Functional motor control deficits in older FMR1 premutation carriers. *Experimental Brain Research*. Retrieved from https://www.ncbi.nlm.nih.gov/pubmed/31161414. doi:10.1007/s00221-019-05566-3

Pincus, S. M., & Goldberger, A. L. (1994). Physiological time-series analysis - what does regularity quantify. *American Journal of Physiology, 266*(4), H1643-H1656. Retrieved from WOS:A1994NJ99600047. doi:10.1152/ajpheart.1994.266.4.H1643

Potter, N. L., Kent, R. D., Lindstrom, M. J., & Lazarus, J. A. (2006). Power and precision grip force control in three-to-five-year-old children: velocity control precedes amplitude control in development. *Experimental Brain Research, 172*(2), 246-260. Retrieved from https://www.ncbi.nlm.nih.gov/pubmed/16432697. doi:10.1007/s00221-005-0322-5

Prablanc, C., & Martin, O. (1992). Automatic control during hand reaching at undetected two-dimensional target displacements. *Journal of Neurophysiology, 67*(2), 455-469. Retrieved from https://www.ncbi.nlm.nih.gov/pubmed/1569469. doi:10.1152/jn.1992.67.2.455

Prodoehl, J., Corcos, D. M., & Vaillancourt, D. E. (2009). Basal ganglia mechanisms underlying precision grip force control. *Neuroscience and Biobehavioral Reviews, 33*(6), 900-908. Retrieved from https://www.ncbi.nlm.nih.gov/pubmed/19428499. doi:10.1016/j.neubiorev.2009.03.004

Przybyla, A., Haaland, K. Y., Bagesteiro, L. B., & Sainburg, R. L. (2011). Motor asymmetry reduction in older adults. *Neuroscience Letters, 489*(2), 99-104. Retrieved from https://www.ncbi.nlm.nih.gov/pubmed/21144883. doi:10.1016/j.neulet.2010.11.074

Raw, R. K., Wilkie, R. M., Culmer, P. R., & Mon-Williams, M. (2012). Reduced motor asymmetry in older adults when manually tracing paths. *Experimental Brain Research, 217*(1), 35-41. Retrieved from WOS:000300580400005. doi:10.1007/s00221-011-2971-x

Reilly, J. L., Lencer, R., Bishop, J. R., Keedy, S., & Sweeney, J. A. (2008). Pharmacological treatment effects on eye movement control. *Brain and Cognition, 68*(3), 415-435. Retrieved from https://www.ncbi.nlm.nih.gov/pubmed/19028266. doi:10.1016/j.bandc.2008.08.026

Rodriguez-Revenga, L., Madrigal, I., Pagonabarraga, J., Xuncla, M., Badenas, C., Kulisevsky, J., . . . Mila, M. (2009). Penetrance of FMR1 premutation associated pathologies in fragile X syndrome families. *European Journal of Human Genetics, 17*(10), 1359-1362. Retrieved from https://www.ncbi.nlm.nih.gov/pubmed/19367323. doi:10.1038/ejhg.2009.51

Roid, G. H. (2003). *Stanford-Binet Intelligence Scales, Fifth Edition: Technical Manual*. Itasca, IL: Riverside Publishing.

Rose, J., & McGill, K. C. (2005). Neuromuscular activation and motor-unit firing characteristics in cerebral palsy. *Developmental Medicine and Child Neurology, 47*(5), 329-336. Retrieved from WOS:000228793300008. doi:10.1017/S0012162205000629

Scaglione, C., Ginestroni, A., Vella, A., Dotti, M. T., Nave, R. D., Rizzo, G., . . . Mascalchi, M. (2008). MRI and SPECT of midbrain and striatal degeneration in fragile X-associated

tremor/ataxia syndrome. *Journal of Neurology, 255*(1), 144-146. Retrieved from https://www.ncbi.nlm.nih.gov/pubmed/18080849. doi:10.1007/s00415-007-0711-8

Schmitz-Hubsch, T., Tezenas du Montcel, S., Baliko, L., Boesch, S., Bonato, S., Fancellu, R., . . . Klockgether, T. (2006). Reliability and validity of the International Cooperative Ataxia Rating Scale: a study in 156 spinocerebellar ataxia patients. *Movement Disorders, 21*(5), 699-704. Retrieved from https://www.ncbi.nlm.nih.gov/pubmed/16450347. doi:10.1002/mds.20781

Schneider, A., Ballinger, E., Chavez, A., Tassone, F., Hagerman, R. J., & Hessl, D. (2012). Prepulse inhibition in patients with fragile X-associated tremor ataxia syndrome. *Neurobiology of Aging, 33*(6), 1045-1053. Retrieved from https://www.ncbi.nlm.nih.gov/pubmed/20961665. doi:10.1016/j.neurobiolaging.2010.09.002

Schoch, B., Regel, J. P., Frings, M., Gerwig, M., Maschke, M., Neuhauser, M., & Timmann, D. (2007). Reliability and validity of ICARS in focal cerebellar lesions. *Movement Disorders, 22*(15), 2162-2169. Retrieved from https://www.ncbi.nlm.nih.gov/pubmed/17712842. doi:10.1002/mds.21543

Shickman, R., Famula, J., Tassone, F., Leehey, M., Ferrer, E., Rivera, S. M., & Hessl, D. (2018). Age- and CGG repeat-related slowing of manual movement in fragile X carriers: A prodrome of fragile X-associated tremor ataxia syndrome? *Movement Disorders, 33*(4), 628-636. Retrieved from https://www.ncbi.nlm.nih.gov/pubmed/29389022. doi:10.1002/mds.27314

Slifkin, A., & Newell, K. M. (1999). Noise, information transmission, and force variability. *Journal of Experimental Psychology-Human Perception and Performance, 25*(3), 837-851. Retrieved from WOS:000080812500016. doi:10.1037/0096-1523.25.3.837

Soontarapornchai, K., Maselli, R., Fenton-Farrell, G., Tassone, F., Hagerman, P. J., Hessl, D., & Hagerman, R. J. (2008). Abnormal nerve conduction features in fragile X premutation carriers. *Archives of Neurology, 65*(4), 495-498. Retrieved from https://www.ncbi.nlm.nih.gov/pubmed/18413472. doi:10.1001/archneur.65.4.495

Stelmach, G. E., & Worringham, C. J. (1988). The preparation and production of isometric force in Parkinson's disease. *Neuropsychologia, 26*(1), 93-103. Retrieved from https://www.ncbi.nlm.nih.gov/pubmed/3362347. doi:10.1016/0028-3932(88)90033-4

Tassone, F., Adams, J., Berry-Kravis, E. M., Cohen, S. S., Brusco, A., Leehey, M. A., . . . Hagerman, P. J. (2007). CGG repeat length correlates with age of onset of motor signs of the fragile X-associated tremor/ataxia syndrome (FXTAS). *American Journal of Medical Genetics. Part B: Neuropsychiatric Genetics, 144B*(4), 566-569. Retrieved from https://www.ncbi.nlm.nih.gov/pubmed/17427188. doi:10.1002/ajmg.b.30482

Trouillas, P., Takayanagi, T., Hallett, M., Currier, R. D., Subramony, S. H., Wessel, K., . . . Manyam, B. (1997). International Cooperative Ataxia Rating Scale for pharmacological assessment of the cerebellar syndrome. The Ataxia Neuropharmacology Committee of the World Federation of Neurology. *Journal of the Neurological Sciences, 145*(2), 205-211. Retrieved from https://www.ncbi.nlm.nih.gov/pubmed/9094050. doi:10.1016/S0022-510X(96)00231-6

Vaillancourt, D. E., & Newell, K. M. (2000). Amplitude changes in the 8-12, 20-25, and 40 Hz oscillations in finger tremor. *Clinical Neurophysiology, 111*(10), 1792-1801. Retrieved from WOS:000089951100011. doi:10.1016/S1388-2457(00)00378-3

Vaillancourt, D. E., Slifkin, A. B., & Newell, K. M. (2001a). Intermittency in the visual control of force in Parkinson's disease. *Experimental Brain Research, 138*(1), 118-127. Retrieved from https://www.ncbi.nlm.nih.gov/pubmed/11374078. doi:https://doi.org/10.1007/s002210100699

Vaillancourt, D. E., Slifkin, A. B., & Newell, K. M. (2001b). Regularity of force tremor in Parkinson's disease. *Clinical Neurophysiology, 112*(9), 1594-1603. Retrieved from https://www.ncbi.nlm.nih.gov/pubmed/11514241. doi:10.1016/S1388-2457(01)00593-4

Vaillancourt, D. E., Slifkin, A. B., & Newell, K. M. (2001c). Visual control of isometric force in Parkinson's disease. *Neuropsychologia, 39*(13), 1410-1418. Retrieved from https://www.ncbi.nlm.nih.gov/pubmed/11585609. doi:10.1016/S0028-3932(01)00061-6

Vaillancourt, D. E., Slifkin, A. B., & Newell, K. M. (2002). Inter-digit individuation and force variability in the precision grip of young, elderly, and Parkinson's disease participants. *Motor Control, 6*(2), 113-128. Retrieved from https://www.ncbi.nlm.nih.gov/pubmed/12122222. doi:10.1123/mcj.6.2.113

Verkerk, A. J., Pieretti, M., Sutcliffe, J. S., Fu, Y. H., Kuhl, D. P., Pizzuti, A., . . . et al. (1991). Identification of a gene (FMR-1) containing a CGG repeat coincident with a breakpoint cluster region exhibiting length variation in fragile X syndrome. *Cell, 65*(5), 905-914. Retrieved from https://www.ncbi.nlm.nih.gov/pubmed/1710175.

Wang, Z., Khemani, P., Schmitt, L. M., Lui, S., & Mosconi, M. W. (2019). Static and dynamic postural control deficits in aging fragile X mental retardation 1 (FMR1) gene premutation carriers. *Journal of Neurodevelopmental Disorders, 11*(1), 2. Retrieved from https://www.ncbi.nlm.nih.gov/pubmed/30665341. doi:10.1186/s11689-018-9261-x

Wang, Z., Kwon, M., Mohanty, S., Schmitt, L. M., White, S. P., Christou, E. A., & Mosconi, M. W. (2017). Increased force variability is associated with altered modulation of the motorneuron pool activity in autism spectrum disorder (ASD). *International Journal of Molecular Sciences, 18*(4). Retrieved from WOS:000402639400024. doi:10.3390/ijms18040698

Wang, Z., Magnon, G. C., White, S. P., Greene, R. K., Vaillancourt, D. E., & Mosconi, M. W. (2015). Individuals with autism spectrum disorder show abnormalities during initial and subsequent phases of precision gripping. *Journal of Neurophysiology, 113*(7), 1989-2001. Retrieved from https://www.ncbi.nlm.nih.gov/pubmed/25552638. doi:10.1152/jn.00661.2014

Yu, S., Pritchard, M., Kremer, E., Lynch, M., Nancarrow, J., Baker, E., . . . et al. (1991). Fragile X genotype characterized by an unstable region of DNA. *Science, 252*(5009), 1179-1181. Retrieved from https://www.ncbi.nlm.nih.gov/pubmed/2031189. doi:10.1126/science.252.5009.1179

Zuhlke, C., Budnik, A., Gehlken, U., Dalski, A., Purmann, S., Naumann, M., . . . Schwinger, E. (2004). FMR1 premutation as a rare cause of late onset ataxia - Evidence for FXTAS in female carriers. *Journal of Neurology, 251*(11), 1418-1419. Retrieved from WOS:000225610400022. doi:10.1007/s00415-004-0558-1